A Bis-Crown Ether Derivative of Triaminotriazine: Synthesis and Behavior of the Ion-Selective and Hydrogen-Bonding Responsive Rotamers

Joe Otsuki, Keith C. Russell, and Jean-Marie Lehn*

Laboratoire de Chimie Supramoléculaire, Université Louis Pasteur, 4, rue Blaise Pascal, 67000 Strasbourg, France

(Received September 6, 1996)

A bis-crown ether derivative of triaminotriazine was synthesized via a phthalic acid derivative of a polyether macrocycle obtained from benzo-18-crown-6. It exists in different conformers distinguishable by ^{1}H NMR at room temperature, in which the macrocyclic side-arms take a closed, half-open, or fully open form, due to the rotational barrier of the C(triazine)–N bond. Large alkali metal ions, such as Rb^+ and Cs^+, the latter being particularly effective, promote the formation of the closed conformer. A barbiturate derivative also causes a similar equilibrium shift to the closed form by establishing complementary hydrogen bonds. The half-open and fully open conformers are induced by smaller alkali metal ions than Rb^+, among which K^+ is the most effective.

Organized supramolecular assemblies, which are incorporated with specific physico-chemical properties, may exhibit a range of novel features distinct from those of the component molecules.[1] 2,4,6-Triaminopyrimidine and barbituric acid derivatives have been found to assemble through complementary hydrogen bonding into organized structures of linear or cyclic type, thus suggesting the possibility to generate regular arrays of units with various properties, e.g. optical, electrical, magnetic, binding, etc., by tethering these units to the hydrogen-bonding components.[2,3] Thus, crown ethers[4] and porphyrins[5] have been assembled by means of a barbiturate derivative. Both assemblies are supramolecular macrocyclic 3 : 3 entities. The assembly including the crown ether derivatized triazine has been characterized by ion-labelling electrospray mass spectrometry, showing that the predominant species is the macrocyclic 3 : 3 hexamer.

We have synthesized a new crown ether derivatized triazine **1**, which was designed so that the macrocyclic rings are arranged in a more or less perpendicular orientation with respect to the plane of the triazine. If this molecule is assembled by means of a barbituric acid derivative into a linear tape structure, a self-assembled solid state model of the ion channel[6] would be generated. In the course of the study, we found that **1** exists in different conformations that have distinct ^{1}H NMR spectra. Furthermore, the distribution of the conformers depend on the size of the added metal ions, owing to the selectivity and complex stoichiometry of the tethered crown ethers. It has also been found that a barbiturate derivative that has complementary hydrogen bonding sites affects the ratio of the conformers. The conformational equilibrium and exchange kinetics may play a role in the process of aggregate formation and growth to macroscopic crystals.

The fact that conformation exchange can be regulated by added chemical species may also be interesting in terms of chemical switches.[1] Examples of substrate-specific structural changes abound in living systems and constitute a basis of processing chemical information.[7] In some enzymes the shape of the active site is modified by the binding of a substrate in an induced-fit mechanism. Allosteric proteins change their structure upon binding with an effector to modify the affinity and/or reactivity towards the substrate. The binding of a specific substance to a receptor protein may change its structure and trigger a subsequent action. Some synthetic compounds are known to take different distinct conformations and change the conformation upon binding to the guest molecule. Calix[4]arenes can adopt four different conformations. Upon the addition of a sodium cation, a tetramethoxycalix[4]arene is fixed in one of the conformations.[8] Other synthetic host compounds exhibiting an induced-fit mechanism have been reported.[9—12]

We report here on the synthesis of compound **1**, its exchange behavior among different conformers, and the effect of metal ions and a barbiturate derivative on it. The structure of **1** is well suited to an analysis of the exchange behavior, since it has only one kind of phenyl protons in each crown arm, making the NMR interpretation straightforward.

Experimental

The melting points were measured on a Mettler FP90-FP82 hot stage. ^{1}H NMR spectra were recorded on a JEOL-GX270 (270 MHz), -JNM-LA (400 MHz), or Brüker-SY200 (200 MHz) spectrometer with Me_4Si as an internal standard. The longitudinal relaxation times were measured on N_2 substituted samples. A total band-shape simulation was conducted on a Macintosh computer using Mathematica software, according to a formulation which was originally developed by Gustowsky et al.,[13] and extended to apply for a system in which four species are exchanging. FTIR spectra were recorded on a Perkin–Elmer 1600 spectrometer.

4′,5′-Bis(chloromethyl)benzo-18-crown-6 2. A mixture of 40% formalin (40 ml) and concd HCl (100 ml) was placed in a three-necked, one-litter flask which was connected to a cylinder of HCl gas. After the initiation of a gas flow, a solution of benzo-18-crown-6 (4.99 g, 16.0 mmol) in concd HCl (200 ml) was slowly added dropwise over a period of 2 h with stirring. The stirring and introducing HCl gas were continued for an additional 15 min. The solution was extracted with CH_2Cl_2 and dried over $MgSO_4$. Evaporation of CH_2Cl_2 afforded a white powder (6.29 g, 96%), mp 117.5—118 °C. ^{1}H NMR ($CDCl_3$) δ_H = 3.6—3.8 (12H), 3.92 (4H, t, J = 4.5 Hz), 4.19 (4H, t, J = 4.5 Hz), 4.67 (4H, s), 6.88 (2H, s). IR (KBr) 2871, 1604, 1526, 1458, 1356, 1284, 1234, 1131, 674, 618 cm^{-1}. FBMS Found: *m/z* 408.1 (M), 431.0 (M+Na). HRMS Found: *m/z* 408.1361. Calcd for $C_{18}H_{26}Cl_2O_6$: M, 408.1156.

4′,5′-Bis(acetoxymethyl)benzo-18-crown-6 3. A mixture of **2** (5.92 g, 14.5 mmol) and AcONa (2.54 g, 3.10 mmol) in glacial AcOH (240 ml) was refluxed with stirring for 6 h. The solution was distilled under reduced pressure to remove most of the solvent. H_2O was then poured into it. Upon extracting with CH_2Cl_2, washing with aqueous $NaHCO_3$ and then H_2O, drying over $MgSO_4$, and evaporating CH_2Cl_2, a white solid (5.82 g, 88%) formed, mp 75.5—76.5 °C. ^{1}H NMR ($CDCl_3$) δ_H = 2.07 (6H, s), 3.65—3.8 (12H), 3.91 (4H, t, J = 4.5 Hz), 4.17 (4H, t, J = 4.5 Hz), 5.10 (4H, s), 6.92 (2H, s). IR (KBr) 2910, 2870, 1729, 1526, 1362, 1265, 1118, 1026, 951, 875 cm^{-1}. FBMS Found: *m/z* 456.2 (M), 479.2 (M+Na). The analytical sample was crystallized from a mixture of ethyl acetate and hexane. Found: C, 57.53; H, 6.99%. Calcd for $C_{22}H_{32}O_{10}$: C, 57.89; H, 7.07%.

4,5-(1,4,7,10,13,16-Hexaoxacyclooctadecano)phthalic Anhydride 4. A mixture of **3** (5.23 g, 11.5 mmol) and 6 M NaOH (100 ml, 1 M = 1 mol dm^{-3}) was heated under reflux and stirred for 5 h. After cooling the solution to 80 °C, a saturated aqueous solution of $KMnO_4$ (5.4 g, 34 mmol) was added in small portions with stirring until a green color persisted for a few minutes. The mixture was stirred for an additonal 1 h at 80 °C. After cooling, the mixture was filtered to remove MnO_2 to give a slightly brown solution, which was acidified with concd HCl to become a yellow solution. After H_2O was evaporated, the resulting white solid was dried under vacuum, which was then heated to 120 °C in Ac_2O for 6 h with stirring. NaCl was removed by filtration, the excess Ac_2O evaporated, and the residue dried under vacuum. The residue was dissolved in a small amount of CH_2Cl_2 to which hexane was added to give two separate phases. The upper white suspension was collected. This procedure of adding hexane and collecting the upper layer was repeated until no more phase separation was observed. Upon evaporation of the solvent from the combined upper layers, white needles (3.31 g, 75%) were obtained, mp 148.5—150.5 °C. ^{1}H NMR ($CDCl_3$) δ_H = 3.65—3.8 (12H), 3.98 (4H, t, J = 4.5 Hz), 4.28 (4H, t, J = 4.5 Hz), 7.32 (2H, s). IR (KBr) 2881, 1845, 1771, 1588, 1507, 1457, 1351, 1326, 1229, 1137, 1112, 986, 890, 738 cm^{-1}. EIMS Found: *m/z* 382 (M). The sample for analysis was crystallized from THF/acetone. Found: C, 56.61; H, 5.85%. Calcd for $C_{18}H_{22}O_9$: C, 56.54; H, 5.80%.

2-Amino-4,6-dihydrazino-1,3,5-triazine 6. A solution of **5** (5.00 g, 30.3 mmol) in MeOH (270 ml) was slowly added dropwise to a mixture of hydrazine hydrate (20 ml) and MeOH (50 ml) with stirring at room temperature. After stirring was continued overnight, a white precipitate (3.83 g, 81%) was collected, washed with methanol, and dried under vacuum, mp 262.5—263 °C. ^{1}H NMR (DMSO) δ_H = 6.24 (2H, br), 7.64 (2H, br). IR (KBr) 3485, 3300, 3176, 1591, 1497, 948, 802, 644 cm^{-1}. FBMS Found: *m/z* 157.1 (M+H). HRMS Found: *m/z*, 156.0877. Calcd for $C_3H_8N_8$: M, 156.0872.

2-Amino-4, 6-bis [[4, 5-[1, 4, 7, 10, 13, 16 -hexaoxacyclooctadecano]-1, 2-benzenedicarboximido]amino]-1,3,5-triazine 1. A mixture of **4** (2.66 g, 6.96 mmol), **6** (1.09 g, 6.96 mmol), and AcOH (0.8 ml) in dioxane (180 ml) was refluxed for 48 h. The solvent was evaporated and the residue dried under vacuum. To the residue were added $(Boc)_2O$ (1.53 g, 7.02 mmol), CH_3CN (30 ml), and DMAP (50 mg, 0.41 mmol). The mixture was stirred at room temperature for 6 h, during which time all of the material went into a red solution. The solvent was evaporated and the red residue was dried under vacuum and then crystallized from MeOH to give soft white needles of **7**, mp > 300 °C. ^{1}H NMR ($CDCl_3$) δ_H = 1.41 (18H, s), 1.43 (18H, s), 3.55—3.8 (24H), 3.97 (8H), 4.22 (8H), 7.14 (4H, s). IR (KBr) 2934, 1747, 1576, 1552, 1505, 1392, 1370, 1307, 1253, 1133, 1048, 850, 755 cm^{-1}.

To purified **7**, TFA was added, and the solution was stirred at room temperature for 3 h. After TFA was evaporated, the yellow residue was suspended in MeOH. MeOH was evaporated and the resulting white powder was suspended in ether, collected by filtration, and dried under vacuum (1.27 g, 41% based on **4**), mp > 300 °C. ^{1}H NMR (DMSO, 100 °C) δ_H = 3.5—3.7 (24H), 3.88 (8H), 4.32 (8H), 7.30 (4H, br) (see Results and Discussion). IR (KBr) 3426, 2922, 1790, 1737, 1598, 1560, 1503, 1452, 1402, 1313, 1223, 1105, 1046, 949, 904, 728, 632 cm^{-1}. FBMS Found *m/z* 885.1 (M+H). Found: C, 51.55; H, 5.68; N, 12.27%. Calcd for $C_{39}H_{48}N_8O_{16}\cdot H_2O$: C, 51.88; H, 5.58; N, 12.41%.

6, 7-(1, 4, 7, 10, 13, 16-Hexaoxacyclooctadecano)-2, 3-dihydrophthalazine-1, 4-dione 8. A solution of **4** (2.21 g, 5.80 mmol), dissolved in glacial AcOH (100 ml) was mixed with $NH_2NH_2\cdot H_2O$ (344 mg, 6.88 mmol) in AcOH (10 ml) and boiled under reflux for 3.5 h. AcOH was evaporated and the residue was dried under vacuum and re-dissolved in CH_2Cl_2/MeOH. Upon slow evaporation of CH_2Cl_2, a white puffy material appeared, which was collected by filtration and crystallized from H_2O to afford white needles (1.73 g, 75%). ^{1}H NMR ($CDCl_3$) δ_H = 3.71 (4H, s), 3.81 (4H, br), 3.94 (4H, br), 4.02 (4H, br), 4.37 (4H, br), 7.36 (2H, br). IR (KBr) 3446, 2878, 1654, 1601, 1516, 1473, 1388, 1285, 1216, 1127, 946, 875, 826, 553 cm^{-1}. EIMS *m/z* 396 (M). HRMS Found: *m/z*, 396.1640. Calcd for $C_{18}H_{24}N_2O_8$: M, 396.1533.

Results and Discussion

Synthesis. The method (Scheme 1) employed to prepare **4**[14] was along the line with the synthesis of 4,5-dimethoxyphthalic acid from 1,2-dimethoxybenzene (veratrole).[15] Bischloromethylation was achieved by slowly dropping a solution of benzocrown ether into a large excess of formaldehyde to prevent the formation of the cyclic trimer[16] and other oligomers. The reaction was quantitative. The diacetoxy compound **3** was obtained quantitatively by treating **2** with sodium acetate. Oxidation of the dialcohol, which was obtained by the hydrolysis of **3**, was most successfully achieved with $KMnO_4$ under a basic condition. Under neutral conditions, however, it seemed that the lactone formed,[17] based on an inspection of ^{1}H NMR spectrum, and further smooth oxidation was prevented. Thus, the basic hydrolysis and the oxidation could be conducted as a one-pot reaction, using 3 molar amounts of $KMnO_4$ with respect to the dialcohol. When a saturated solution of $KMnO_4$ was added to a hot solution of the dialcohol while the oxidation reaction was taking place, the color of permanganate turned green, but soon faded

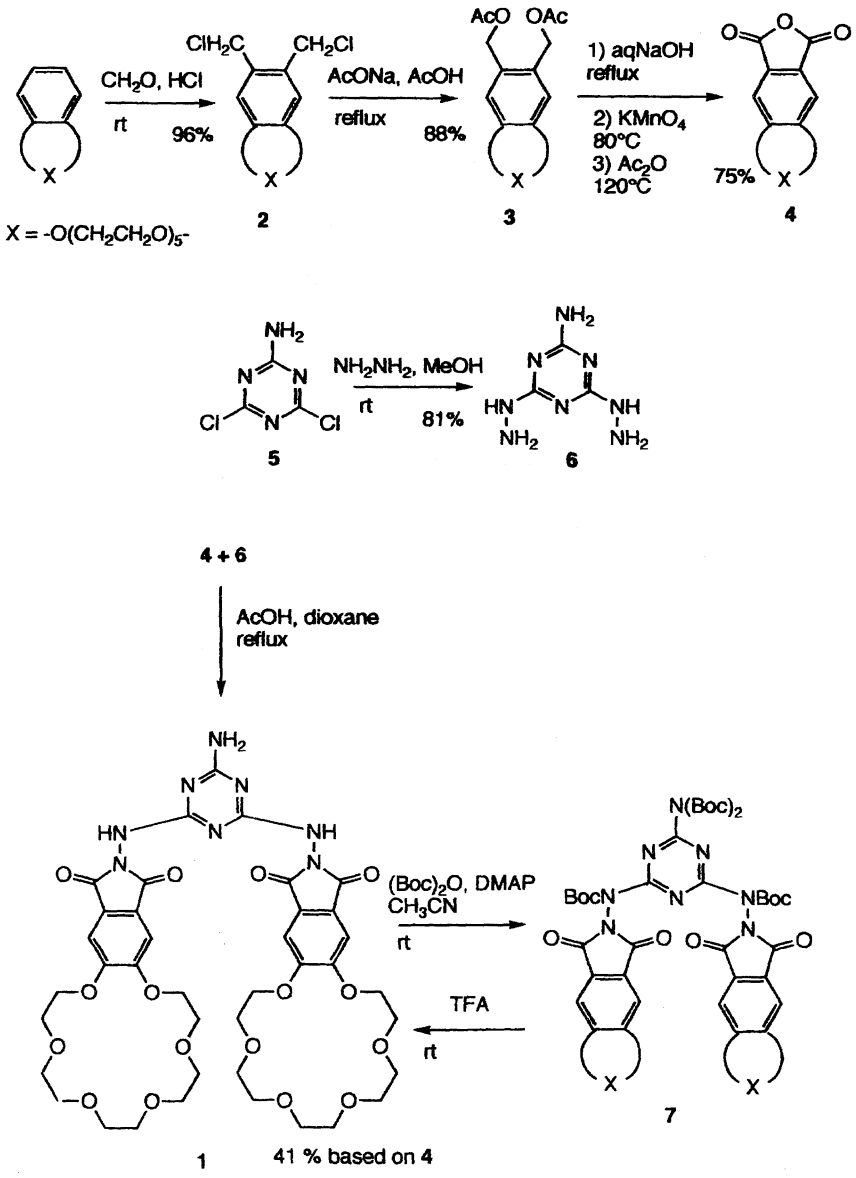

Scheme 1.

away. When the reaction was completed, the color persisted for several minutes before fading away. The diacid can be converted to the anhydride **4** either with acetic anhydride[18] or thionyl chloride. Thus, the phthalic anhydride derivative of benzocrown ether was prepared by an efficient synthetic route. The anhydride may be a useful handle to attach crown ethers to other chemical species, such as polymers.

Two possibilities were considered for connecting the triazine and the macrocycles through hydrazine, depending on whether hydrazine was first attached to the triazine to give **6** or to the macrocycle as aminoimide. As a model of the latter approach, *N*-aminophthalimide and **5** were allowed to react overnight in refluxing dioxane, but only the starting materials were recovered in the reaction mixture. The *N*-amino group in *N*-aminophthalimide seems not to be a good enough nucleophile, unlike hydrazine. On the other hand, **6** reacted with phthalic anhydride to afford the diimide. Hence, the reaction scheme via **6** was the route of choice.

The subtle nature of the reaction of the dihydrazine **6** and the anhydride **4** is that the production of the desired aminoimide **1** may be in competition with that of the hydrazide. The reaction proceeds in two-steps. The first step is the reaction of the phthalic anhydride with the primary amine of **6** to make an amide bond. The second step has two cyclization possibilities: one is to the five-membered ring aminoimide; the other is to the six-membered ring hydrazide (Chart 1). The simple reaction between hydrazine and phthalic anhydride favors the formation of a six-membered ring.[19] The aminoimide structure should show only one singlet of the ^{1}H NMR spectrum in the aromatic region, whereas the hydrazide structure should show two singlets. The complex ^{1}H NMR spectrum at room temperature (Fig. 1, top), especially that for the aromatic region (as detailed later), was puzzling at first glance. The spectrum at 100 °C (Fig. 1, bottom), however, agreed with the aminoimide structure. The C=O stretching band at 1737 cm^{-1} in the IR spectrum

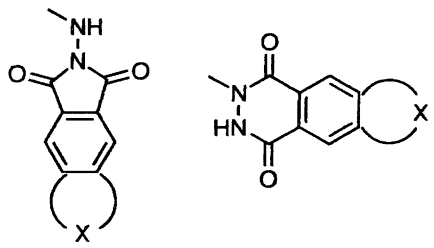

Chart 1.

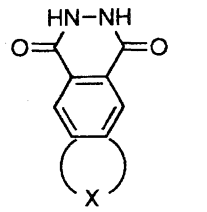

8

Chart 2.

of **1** also supports the assumed aminoimide structure; it is close to that of *N*-aminophthalimide[20] at 1729 cm^{-1}, while phthalhydrazide[20] and **8** (Chart 2), which was obtained from **4** and hydrazine, show bands at 1663 and 1654 cm^{-1}, respectively. In the present case, since the triazine ring reduces the nucleophilicity of the directly attached N site of hydrazine, the aminoimide formation is favored.

The crude product **1** was purified after introducing Boc groups on all of the NH sites in order to make the product more soluble and easy to handle. The purified product was deprotected by a treatment with TFA to afford the final compound **1**.

Rotameric Forms of Compound 1. The ^{1}H NMR spectrum of **1** shows four peaks in the aromatic region in DMSO-d_6 at room temperature, as described briefly above (Fig. 1, top). A similar splitting was observed in dioxane-

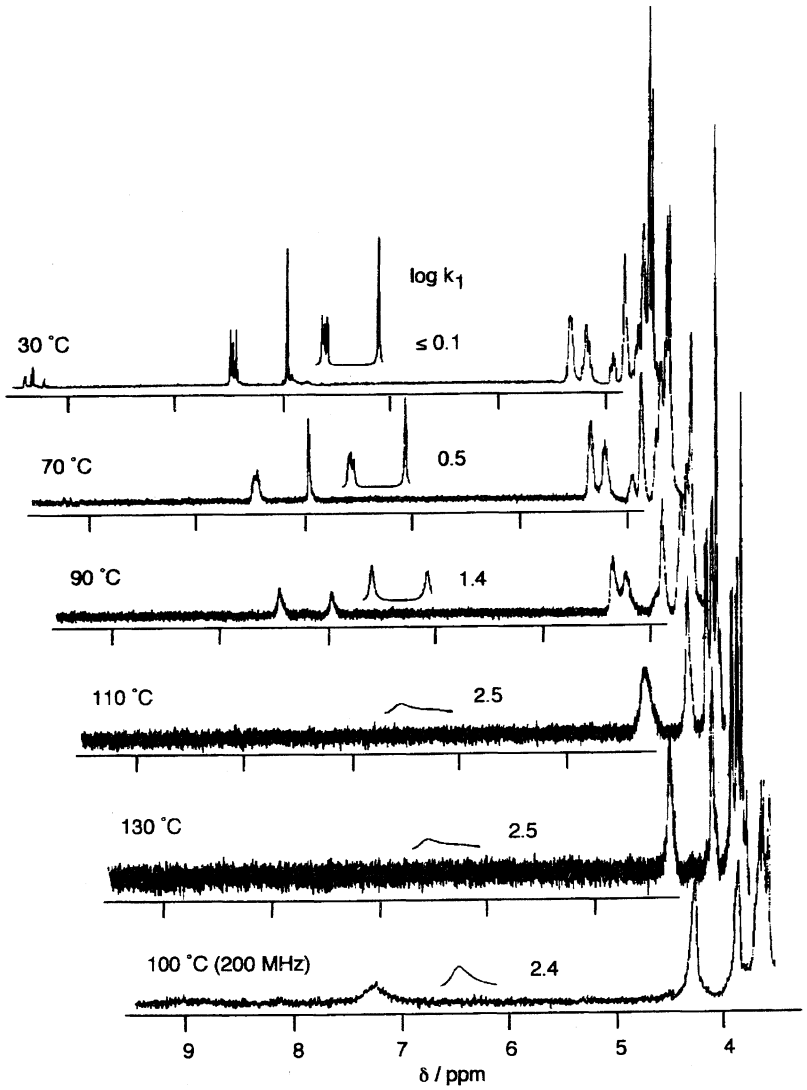

Fig. 1. ^{1}H NMR spectra of **1** (1 mM) in DMSO-d_6 at different temperatures at 400 MHz except for the spectrum at the bottom. Included also are results of the total bandshape simulation based on the scheme in Fig. 3 using log k_1 values indicated.

d_8. Also, the peaks of the oxyethylene chains are complex, and not of the typical [4H; 4H; 12H] pattern of benzo-18-crown-6 ether observed for compounds **2**—**4**. It was thought that these features might be due to the presence of rotational isomers, as was proven to be correct by high-temperature NMR measurements. Indeed, the peaks converge to one broad peak at 100 °C (200 MHz; Fig. 1, bottom). At this temperature, the proton signals of the polyether part are simplified to the expected [4H; 4H; 12H] pattern. There are three possible rotational isomers which can account for the observed peaks: closed, half-open, and fully open conformers (Fig. 2). The upper-field peak at 6.97 ppm arises from the closed conformer, considering the ring-current effect of the benzene ring, while the lower-field peaks are due to the half-open (7.46 and 7.51 ppm) and fully open (7.49 ppm) forms. These latter two conformers are hereafter called open conformers. The Boc derivatized compound **7** exhibits only one singlet peak at 7.1 ppm and the [4H; 4H; 12H] pattern for the oxyethylene chain. The same is true for the model compound **9**, the bis-phthalimide which does not contain the macrocycles present in **1**. The ^{1}H NMR spectrum of **9** shows a pair of symmetrical peaks around 7.5 ppm and unsymmetrical peaks at 7.9—8.0 ppm. This is also in accord with the picture in Fig. 2. The symmetrical peaks at the higher magnetic field can be assigned to the closed conformer and the lower field unsymmetrical peaks to the open conformers. Introducing Boc groups to **9** gives a product whose spectrum showed only a pair of symmetrical peaks. In this case also, the rotational barrier becomes lower when the amino protons are substituted by Boc groups.

The first flip around one C(triazine)–N bond of closed conformer gives a half-open conformer, and the second flip of the other C(triazine)–N bond gives a fully open conformer.

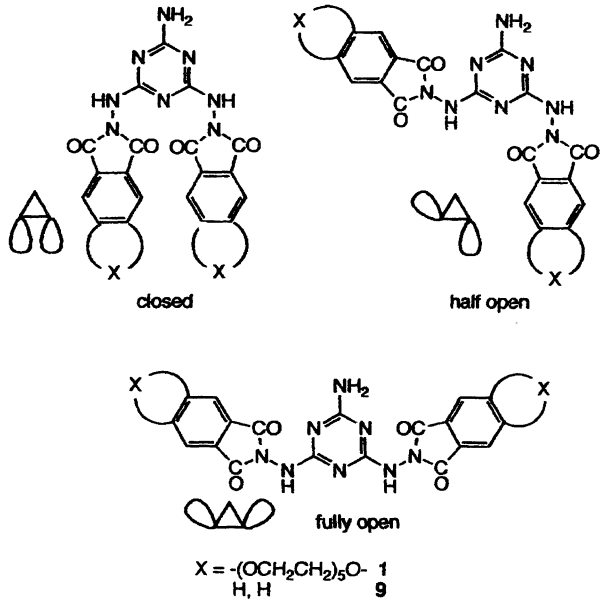

Fig. 2. Three kinds of rotamers of **1** and **9** which exist in solution and their schematic representation used in other figures.

The equilibrium is depicted in Fig. 3. From the fractions of protons in the ^{1}H NMR spectrum, the equilibrium constants, which are the ratios of the relevant rate constants, are derived as $k_2/k_1 = 2.8$ and $k_4/k_3 = 1.3$. An estimation of the value of k_1 at 30 °C was attempted by ^{1}H NMR magnetization transfer experiments. However, the selective irradiation of the protons of the open conformers at around 7.5 ppm had no effect on the intensity of the proton peak of the closed conformer at 6.97 ppm. This indicates that the lifetime of the closed conformer, defined as k_1^{-1}, is much longer than the longitudinal relaxation time of the proton of the closed conformer, which is 0.84 s. This sets the upper limit for k_1 as $k_1 \ll 1.2$ s^{-1} and the lower limit for the corresponding activation free energy as $\Delta G^{\ddagger}_1 > 74$ kJ mol^{-1}.

The rate constants of the conformational exchange and the activation free energies for the rotational barrier were estimated at higher temperatures by a total band-shape analysis[13] using the aromatic proton peaks. In the calculation, k_3 was assumed to be equal to k_1 to reduce the number of parameters. Thus, the only parameter to be adjusted was k_1. This simplification may be justified since the line shape is relatively insensitive to the variation of k_3. The results of the simulation of the line-shape are included in Fig. 1 together with the determined values of $\log k_1$ by fitting to the observed spectra. The errors in the values were estimated to be ±0.5 for $\log k_1$. These k_1 values give an activation free energy ($\Delta G^{\ddagger}_1$) of 75—81 kJ mol^{-1} for rotation around the C(triazine)–N bond. This is comparable to values for a hindered rotation around single bonds with a partial double-bond character. A well-known example of this kind is the C(=O)–N bond of *N*,*N*-dimethylformamide derivatives. Values ranging from 51 to 86 kJ mol^{-1} have been reported for the barriers to rotation in amides, depending on the substituents.[21] The rotation around the bond between an amino nitrogen and a ring carbon of nitrogen-containing heterocycles, such as aminopyrimidine derivatives, is known to have relatively high barriers.[22]

Effects of Ions on the Rotameric Equilibria in Compound 1. Benzo-18-crown-6 derivatives are known to form a 1 : 1 complex with alkali metal ions with a preference for K^+.[23,24] On the other hand, larger metal ions, e.g. Rb^+ and Cs^+, form a sandwich type 1 : 2 complex involving two macrocycles.[23,25] Bis-crown ethers are especially effective for trapping these large metal ions.[26] The crystal structure of the sandwich complex between a bis-crown ether having a structure similar to **1** and Rb^+ has appeared.[27] Consequently,

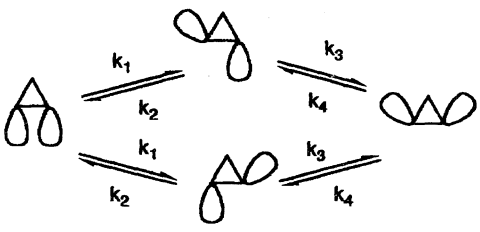

Fig. 3. Schematic representation of the conformational exchange processes among different rotamers.

we investigated the interaction of **1** with a series of alkali metals and the effect of the metal ions on the conformers.

Representative examples of the ^{1}H NMR spectral change upon the addition of alkali metal ions to **1** in DMSO are shown in Fig. 4. When K^+ is added, both peaks of the open and closed conformers are shifted downfield, due to complex formation. In addition to the shift, the fraction of open conformers increases. On the other hand, the addition of a larger alkali metal ion, Cs^+, results in a nearly total conversion to the closed conformer. The downfield shift of the peak of the closed conformer is larger than that in the K^+ case. This spectral change indicates a strong preference of Cs^+ for the closed conformer over open ones.

The magnitude of the downfield shift is a function of the amount and limiting chemical shift of the complex, and may be a measure of the strength of the interaction between the crown ether and metal ions. The chemical shift changes upon the addition of metal ions are summarized in Table 1. Small ions, such as Li^+ and Na^+, and divalent Ca^{2+} cause only small shifts, which indicates that the interactions of the crown ether and these metals are very weak. When 30 mM of K^+ is added, the signals of both the open and closed conformers experience a downfield shift of ca. 0.1 ppm, which indicates that complexation takes place. The similar magnitudes of the downfield shifts for the open and closed conformers suggest that there is little preference of K^+ for a particular conformer. On the other hand, when the larger Rb^+ ion is added, the magnitude of the downfield shift for the closed conformer is twice that for the open conformers. This is more so for the even larger Cs^+; the magnitude of the downfield shift for the closed conformer is 4-times that for the open conformers. Thus, these large alkali metal ions favor the closed conformer, strongly suggesting that sandwich-type complexes are formed between **1** and these ions.

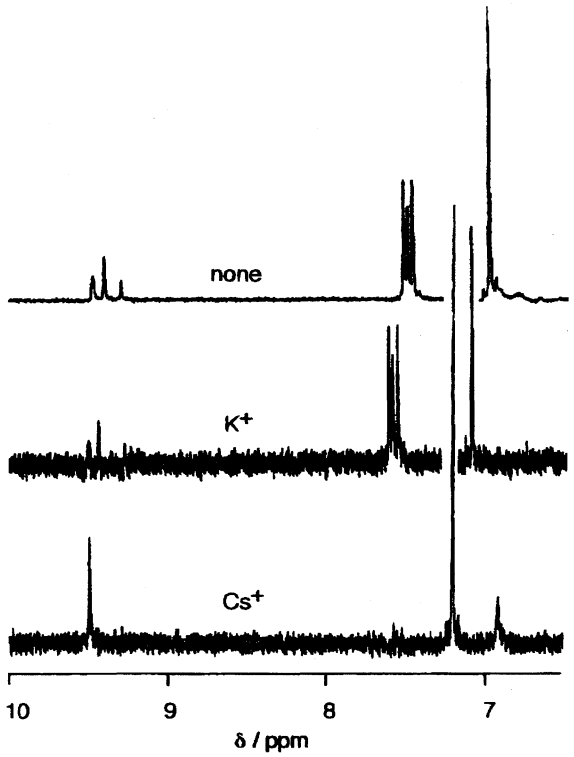

Fig. 4. ^{1}H NMR spectra of solutions of 1 mM of **1** and 30 mM of metal ions in DMSO-d_6 at 30 °C. Peaks above 9 ppm and at 6.9 ppm (bottom) are of NH active protons.

Figure 5 shows the fractions of the open and closed conformers in the presence of 30 mM of metal perchlorate in DMSO at 30 °C. An increase in the formation of the open conformers takes place upon the addition of Li^+, Na^+, K^+, and Ca^{2+}, more or less in parallel with the expected affinity of 18-crown-6 macrocycles for these ions. It is possible, especially when K^+ is present in excess, that the accommodation of an ion in each of the crown ethers of **1** introduces an electrostatic repulsion between these positive charges, thus shifting the equilibrium towards the open conformers where these complexed sites are far apart.

Since the effect of Cs^+ was the most pronounced, we examined the equilibrium shift as a function of the concentration of Cs^+ in more detail. Figures 6a and 6b show titration curves of the chemical shifts and the population ratio, respectively, of the open and closed conformers. The change in the chemical shift of the closed conformer saturates at as low as 5 mM of Cs^+, while the curve indicates that the open ones are still at low loading levels at up to 30 mM of Cs^+. Concomitant with the changes in the chemical shifts, the amount of closed conformer increases upon an increase in Cs^+ concentration. The equilibria in this system can be depicted as shown in Fig. 6c. Interconversion of the open and closed conformations and metal complexation and decomplexation processes are involved in the equilibria. The association constants for the complexation of **1** with Cs^+, determined from the data in Fig. 6a for the open (K_a^o) and closed (K_a^c) conformers, are 58 ± 5 M^{-1} and 2800 ± 70 M^{-1}, respectively, indicating a strong preference of Cs^+ to the closed conformer over the open one. From these association constants and the population ratio of the closed over open conformers ($K_{c/o}$) in the absence of added metal ions, which happens to be unity, the population ratio for the com-

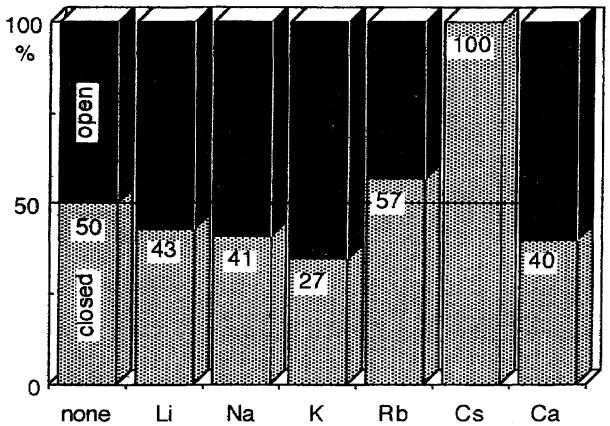

Fig. 5. Fractions of the open and closed conformers in solutions of 1 mM of **1** in the presence of 30 mM of metal ions in DMSO-d_6 at 30 °C.

Table 1. Ion Induced ^{1}H NMR Chemical Shift Changes in DMSO at 30 °C

Cation	Concn	δ_{open}			$\Delta\delta_{open}$[a,b]	δ_{closed}	$\Delta\delta_{closed}$[a]
	mM	ppm	ppm	ppm	ppm	ppm	ppm
None		7.51	7.49	7.46		6.97	
Li	30	7.51	7.48	7.45	−0.01	6.97	0.00
Na	30	7.53	7.50	7.47	0.01	6.99	0.02
K	30	7.61	7.58	7.55	0.09	7.09	0.12
	100	7.62	7.59	7.56	0.10	7.11	0.14
Rb	30	7.60	7.57	7.54	0.08	7.13	0.16
Cs	30	7.57	7.55	7.52	0.06	7.20	0.23
Ca	30	7.49	7.47	7.44	−0.02	6.95	−0.02

a) A downfield shift is taken as positive. b) The averages of the three resonances are given.

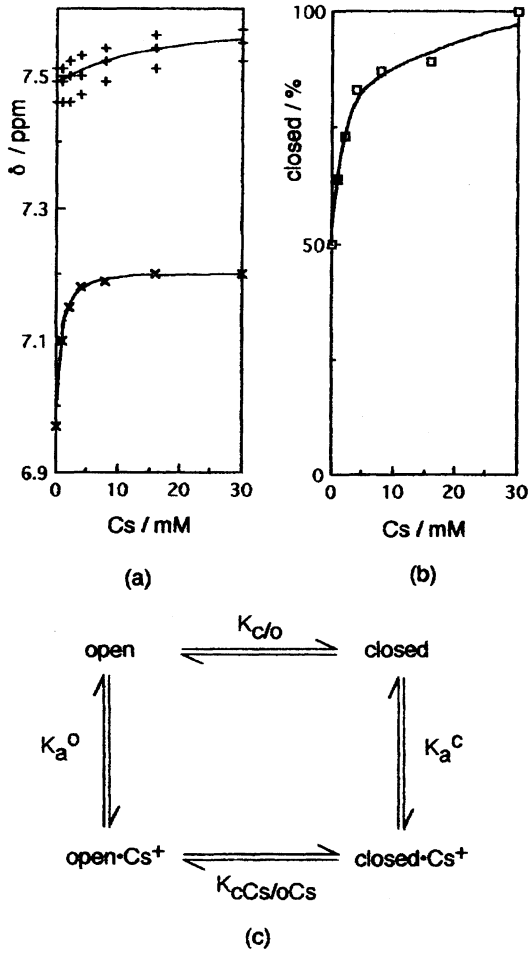

Fig. 6. The effect of the concentration of Cs^+ on the chemical shifts of **1** (a) and the population ratio of the closed conformer (b) and the underlying equilibria (c).

plexed species, $K_{cCs/oCs}$=[open·Cs^+]/[closed·Cs^+], is derived to be 48. Thus, the sandwich-type complex comprising two macrocycles and a metal ion is preferred ca. 50 times over a complex involving only one macrocycle.

Figure 7 schematically illustrates what is happening upon the addition of K^+ and Cs^+. In the absence of metal ions, the open and closed conformers exists in the ratio of 1 : 1. The addition of K^+ leads firstly to the formation of a 1 : 1

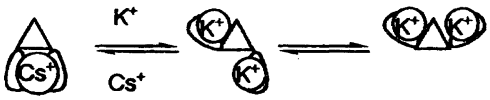

Fig. 7. Schematic representation of the specific effect of the binding of K^+ and Cs^+ to the conformers.

complex, and then to a certain amount of a 2 : 1 complex in the presence of excess K^+, thus causing an increase of the open conformers. When Cs^+ is added, the equilibrium is shifted predominantly towards the closed conformer to form the sandwich-type complex.

Effect of Hydrogen Bonding to a Complementary Barbituric Acid Derivative on the Rotameric Equilibrium of Compound 1. The bis-crown compound **1** is not soluble in chloroform by itself. However, it is solubilized by the addition of more than 2 molar amounts of **10** (Chart 3), a barbiturate derivative bearing two long alkyl chains. The head group of **10** has hydrogen bonding sites complementary to those of **1**. For a slightly turbid solution of 1 mM of **1** and 2 mM of **10** in $CDCl_3$, two phenyl proton peaks are observed at 6.9 and 7.1 ppm in the ^{1}H NMR spectrum (Fig. 8a). By comparison with the spectra in DMSO, the higher field peak is assigned to the protons of the closed conformer and the lower field one to those of the open ones. A further addition of **10** results in an increase of the closed conformer (Fig. 8b), finally leading to a nearly complete conversion to the closed conformer (Fig. 8c). These observations indicate that the closed conformer dominates when excess **10** is present, due to the establishment of three-point hydrogen-bonding interactions between **10** and the closed conformer of **1**, as shown in Fig. 9. When the three-point hydrogen bonds form, the crown unit is forced away from **10** to lead to the closed conformer.

The peak of the NH proton of **10** observed above 8 ppm is a

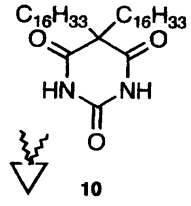

Chart 3.

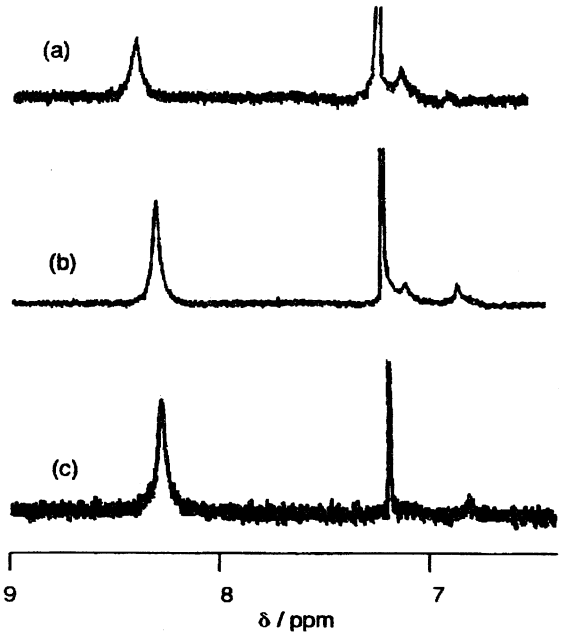

Fig. 8. ^{1}H NMR spectra of mixtures of 1 mM of **1** and 2 (a), 4 (b), and 8 (c) mM of **10** in $CDCl_3$ at room temperature. The peak at 7.25 ppm is of the residual $CHCl_3$ and that above 8 ppm is of the NH protons of **10**.

good indicator of hydrogen bonding involving the barbiturate NH. It is notable that it is observed at the lowest field for the sample including the smallest amount of **10** (Fig. 8a). It follows that hydrogen bonding between **1** and **10** is preferred over binding of **10** with itself. This highlights the importance of the complementarity of hydrogen bonds.

Attempts to observe a synergistic effect of metal ions and complementary hydrogen bonding on the conformational equilibrium of **1** has not succeeded. This is because **1**, solubilized with the formation of hydrogen bonds with **10** in chloroform, precipitates out of solution upon the addition of metal salts, while hydrogen bonds are not formed in more polar solvents, such as DMSO, in which metal ions are effective in switching the conformational equilibrium of **1**.

Conclusion

We synthesized a hydrogen bonding assembler **1** bearing two macrocycles. Due to the rotational barrier of the C(triazine)–N bond, **1** exists in different conformations which give distinctive ^{1}H NMR signals. The equilibrium among these conformers can be shifted by the addition of alkali metal ions. Especially, Cs^+, the largest ion among studied, is particularly effective; total conversion to the closed conformer is achieved. A barbiturate derivative **10**, which has hydrogen bonding sites complementary to **1**, exerts a similar effect to switch the conformation to the closed conformer. As pointed out in the introduction, the conformational exchange may play a role in the assembling process. A further characterization of multicomponent supramolecular species involving metal ions and hydrogen-bonding assemblers bearing macrocycles is in progress.

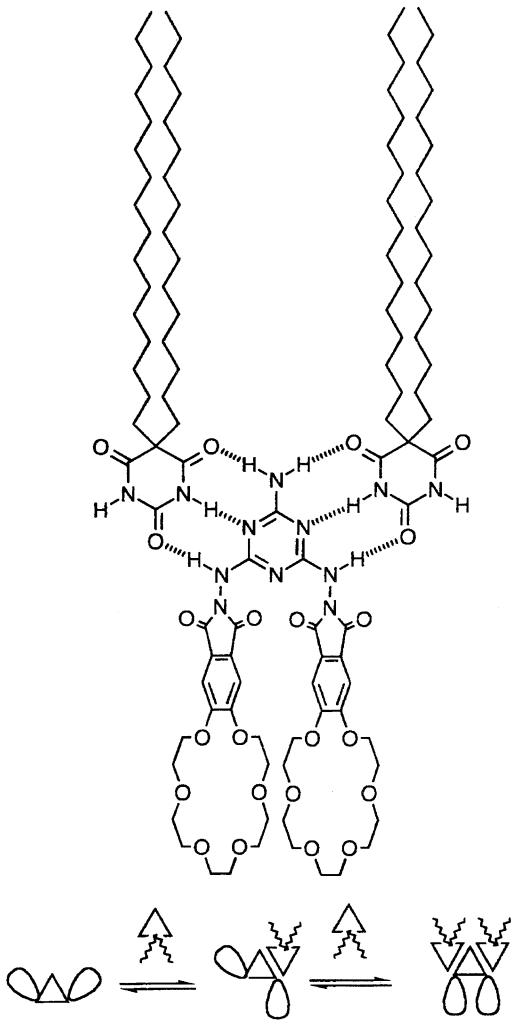

Fig. 9. Formation of complementary three point hydrogen bonding arrays between **1** and **10** and schematic representation of its effect on the conformation of **1**.

We thank Prof. K. Araki of the University of Tokyo for helpful discussions. HRMS was taken by Prof. H. Tomoda of the Shibaura Institute of Technology. Post-doctoral fellowships from the Canon Foundation in Europe (J. O.) and the Collège de France (K. C. R.) are gratefully acknowledged.

References

1) a) J.-M. Lehn, "Supramolecular Chemistry," VCH, Weinheim (1995); b) J.-M. Lehn, *Angew. Chem., Int. Ed. Engl.*, **29**, 1304 (1990).

2) a) J.-M. Lehn, M. Mascal, A. Decian, and J. Fischer, *J. Chem. Soc., Chem. Commun.*, **1990**, 479; b) J.-M. Lehn, M. Mascal, A. Decian, and J. Fischer, *J. Chem. Soc., Perkin Trans. 2*, **1992**, 461.

3) a) G. M. Whitesides, E. C. Simanek, J. P. Mathias, C. T. Seto, D. N. Chin, M. Mammen, and D. M. Gordon, *Acc. Chem. Res.*, **28**, 37 (1995); b) J. C. MacDonald and G. M. Whitesides, *Chem. Rev.*, **94**, 2383 (1994).

4) K. C. Russell, E. Leize, A. V. Dorsselaer, and J.-M. Lehn,

Angew. Chem., Int. Ed. Engl., **34**, 209 (1995).

5) C. M. Drain, K. C. Russell, and J.-M. Lehn, *J. Chem. Soc., Chem. Commun.*, **1996**, 337.

6) a), J.-P. Behr, J.-M. Lehn, A.-C. Dock, and D. Mora, *Nature*, **295**, 526 (1982); b) A.-C. Dock, D. Moras, J.-P. Behr, and J.-M. Lehn, *Acta Crystallogr., Sect. C*, **C39**, 1001 (1983).

7) L. Stryer, "Biochemistry," 2nd ed, Freeman, New York (1981).

8) a) J. Blixt and C. Detellier, *J. Am. Chem. Soc.*, **117**, 8536 (1995); b) J. Blixt and C. Detellier, *J. Am. Chem. Soc.*, **116**, 11957 (1994).

9) P. D. Beer and A. S. Rothin, *J. Chem. Soc., Chem. Commun.*, **1988**, 52.

10) Y. Murakami, J. Kikuchi, T. Ohno, O. Hayashida, and M. Kojima, *J. Am. Chem. Soc.*, **112**, 7672 (1990).

11) J. C. Adrian, Jr., and C. S. Wilcox, *J. Am. Chem. Soc.*, **114**, 1398 (1992).

12) R. P. Sijbesma and R. J. M. Nolte, *J. Am. Chem. Soc.*, **113**, 6695 (1991).

13) a) H. S. Gustowsky and C. H. Holm, *J. Chem. Phys.*, **25**, 1228 (1956); b) H. S. Gustowsky and A. Saika, *J. Chem. Phys.*, **21**, 1668 (1953); c) H. S. Gustowsky, D. W. McCall, and C. P. Slichter, *J. Chem. Phys.*, **21**, 279 (1953).

14) The crystal structure of the phthalic acid derivative of benzocrown ether (the precursor of **4**) has appeared. However, no description on the synthesis has been given: a) F. Benetollo, *J. Inclusion Phenom.*, **5**, 165 (1987); b) F. Benetollo, G. Bombieri, and M. R. Truter, *J. Heterocycl. Chem.*, **26**, 981 (1989).

15) J. H. Wood, M. A. Perry, and C. C. Tung, *J. Am. Chem. Soc.*, **72**, 2989 (1950).

16) A. Collet, *Tetrahedron*, **43**, 5725 (1987).

17) V. I. Stenberg and R. J. Perkins, *J. Org. Chem.*, **28**, 323 (1963).

18) B. H. Nicolet and J. A. Bender, *Org. Synth.*, Coll. Vol. 1, 410 (1967).

19) H. D. K. Drew and H. H. Hatt, *J. Chem. Soc.*, **1937**, 16.

20) J. Gut, A. Novacek, and P. Fiedler, *Collect. Czech. Chem. Commun.*, **33**, 2087 (1968).

21) M. Oki, *Top. Stereochem.*, **14**, 1 (1983).

22) M. Oki, "Applications of Dynamic NMR Spectroscopy to Organic Chemistry, Methods in Stereochemical Analysis," VCH, Weinheim (1985), Vol. 4.

23) J. J. Christensen, D. J. Eatough, and R. M. Izatt, *Chem. Rev.*, **74**, 351 (1974).

24) S. Kopolow, T. E. H. Esch, and J. Smid, *Macromolecules*, **4**, 359 (1971).

25) C. J. Pedersen, *J. Am. Chem. Soc.*, **92**, 386 (1970).

26) K. Kimura, H. Tamura, and T. Shono, *J. Chem. Soc., Chem. Commun.*, **1983**, 492.

27) L. Zhang, T. Lu, B. Luo, Z. Shao-Hui, and H. Hu, *Supramol. Chem.*, **1**, 107 (1993).